Submitted to Journal of Low
Temperature Physics

LBL-2567
Preprint

MAGNETIC FOCUSING OF ELECTRONS AND HOLES IN BISMUTH

RECEIVED
LAWRENCE
RADIATION LABORATORY

MAR 20 1974

LIBRARY AND
DOCUMENTS SECTION

John Clarke and Louis A. Schwartzkopf

January 1974

Prepared for the U. S. Atomic Energy Commission
under Contract W-7405-ENG-48

TWO-WEEK LOAN COPY

This is a Library Circulating Copy which may be borrowed for two weeks. For a personal retention copy, call Tech. Info. Division, Ext. 5545

LAWRENCE BERKELEY LABORATORY
UNIVERSITY OF CALIFORNIA
BERKELEY

LBL-2567

DISCLAIMER

This document was prepared as an account of work sponsored by the United States Government. While this document is believed to contain correct information, neither the United States Government nor any agency thereof, nor the Regents of the University of California, nor any of their employees, makes any warranty, express or implied, or assumes any legal responsibility for the accuracy, completeness, or usefulness of any information, apparatus, product, or process disclosed, or represents that its use would not infringe privately owned rights. Reference herein to any specific commercial product, process, or service by its trade name, trademark, manufacturer, or otherwise, does not necessarily constitute or imply its endorsement, recommendation, or favoring by the United States Government or any agency thereof, or the Regents of the University of California. The views and opinions of authors expressed herein do not necessarily state or reflect those of the United States Government or any agency thereof or the Regents of the University of California.

Submitted to Journal of Low Temperature Physics

LBL-2567
Preprint

UNIVERSITY OF CALIFORNIA

Lawrence Berkeley Laboratory
Berkeley, California

AEC Contract No. W-7405-eng-48

MAGNETIC FOCUSING OF ELECTRONS AND HOLES IN BISMUTH*

John Clarke and Louis A. Schwartzkopf

JANUARY 1974

Magnetic Focusing of Electrons and Holes In Bismuth*

John Clarke† and Louis A. Schwartzkopf‡

Department of Physics, University of California,
and
Inorganic Materials Research Division,
Lawrence Berkeley Laboratory,
Berkeley, California 94720

* Work supported by the U. S. Atomic Energy Commission.

† Alfred P. Sloan Foundation Fellow.

‡ Present address: Dept. of Physics, Rutgers Univ., New Brunswick, N.J.

ABSTRACT

The electron and hole focusing effects in a magnetic field predicted by Pippard have been observed in bismuth. Two interlocking superconducting combs were evaporated onto the surface of a bismuth single crystal. The resistance R(H) between the combs was measured with a superconducting voltmeter as a function of the magnetic field H applied parallel to the teeth of the combs. A local minimum in the resistance was observed when the magnetic field focused electrons or holes in extremal

orbits between the teeth of different combs. A similar effect was observed when the combs were replaced by two parallel superconducting strips. In this case, the dependence of R(H) on H was in good qualitative agreement with the calculation of Gonçalves da Silva on a model whose Fermi surface was topologically equivalent to that of bismuth. From the values of H at which the minima occurred, we have deduced estimates for D_{xe} and D_{ze}, the diameters of the principal electron ellipsoid along the binary and trigonal axes. We find $D_{xe} = (0.94 \pm 0.03) \times 10^{-2}$ Å^{-1} and $D_{ze} = (1.35 \pm 0.04) \times 10^{-2}$ Å^{-1}. These values lie somewhat below other values in the literature. This discrepancy may occur because each minimum in R(H) occurs at a field slightly below H_o, where H_o is the field for which the diameter of the extremal electron trajectory is equal to the separation of the superconducting strips.

1. INTRODUCTION

In an appendix to a paper by Hawkins, Pippard[1] proposed a new type of focusing experiment in metals. In this article, we report the first observation of the focusing effect, in bismuth. The experimental results are used to estimate two diameters of the Fermi surface.

Pippard's proposed geometry[1] is shown in Fig. 1. The specimen is a single crystal of normal metal with a long mean free path ℓ. Superconducting strips are evaporated onto a plane surface of the specimen; alternate strips are connected to form two interlocking combs. The separation of the midpoints of adjacent strips is d ($< \ell$). The resistance R(H) between the combs is measured at constant current as a function of a uniform magnetic field H applied parallel to the teeth of the combs. If the Fermi surface of the metal is a sphere, the electron trajectories in real space will be circular helices with diameters inversely proportional to the magnetic field. At the magnetic field H_o for which the diameter of the extremal electron trajectory in real space is equal to d, R(H) is expected to have a local minimum $R(H_o)$. In general, local minima are expected at $H = H_o/(2n-1)$, where $n = 1,2,3 \ldots$. For non-spherical Fermi surfaces, we still expect local minima when the extremal diameter (the diameter of the extremal trajectory) of the real-space orbit is equal to (2n-1)d. The trajectories in real space projected onto the plane perpendicular to $\vec{H}$ have the same shape as those in k-space, but are scaled by a factor of $\hbar c/eH$ and rotated through $\pi/2$ about $\vec{H}$. The primary (n=1) focusing condition in k-space is

$$D = eH_o d/\hbar c, \tag{1}$$

where D is the extremal diameter of the Fermi surface in the direction perpendicular to the specimen surface. For a complex Fermi surface consisting of several sheets, we expect a minimum corresponding to the extremal diameter of each sheet.

Gonçalves da Silva[2] has calculated the resistance R(H) between two superconducting strips on the sample surface. In his model, he assumes zero temperature, that the current distribution across the strips is uniform, and that all surface scattering is diffuse. He also assumes there is a resistive layer[1] of infinitesimal thickness on the surface of the crystal, between the metal and the superconducting strips. This crucial assumption allows the potential to vary along the surface of the crystal from one side to the other of each superconducting strip. Gonçalves da Silva calculates R(H) for the two limits $\ell \gg d$, and $\ell \ll d$, and for several models of the Fermi surface. In particular, for $\ell \gg d$ he considers a compensated Fermi surface consisting of one hole sphere and three equal electron spheres: this model is topologically equivalent to the Fermi surface of bismuth. He finds a minimum corresponding to the diameter of the electron spheres. However, the minimum occurs at a field $H_m < H_o$. The ratio H_m/H_o depends on w/d, where w is the width of the superconducting strips, and approaches 1 as w/d tends to zero. There is no minimum corresponding to the larger diameter of the hole sphere, but a shoulder associated with this diameter appears in R(H) as w/d tends to zero.

This experiment is related to other size effect experiments, such

as cyclotron resonance cut-off,[3] the radio-frequency size effect,[4] and the magneto-acoustic effect.[5] These techniques also measure linear dimensions of the Fermi surface by relating the shape of an orbit in real space to the shape in k-space. However, our focusing experiment determines extremal diameters, whereas the other experiments measure extremal calipers. (An extremal caliper is the separation of the two parallel planes between which the extremal cross section of the Fermi surface just fits.)

In section 2, we describe the experimental procedures, and in section 3, we briefly review the Fermi surface of bismuth. We present the results in section 4, and an analysis of the results in section 5. Section 6 contains a summary, and suggestions for further work.

2. EXPERIMENTAL METHODS

2.1 Choice of Materials

Bismuth was chosen because of the small diameters of its electron and hole Fermi surfaces. Orbits that satisfy the criterion $\omega_c\tau \gg 1$ (ω_c is the cyclotron frequency and τ the relaxation time) can be obtained in fields of only a few G. The use of such low fields greatly reduced transient currents generated in the detection circuit by vibration of the sample in the magnetic field. Bismuth is easy to grow in single crystals and has a well-characterized Fermi surface. Tin was used for the superconducting strips because of its relatively low solubility in bismuth compared with lead and indium.

2.2 Sample Preparation

The starting material was 99.9999% bismuth obtained from Consolidated Mining and Smelting Company of Canada, Limited. We melted the bismuth

in a vertical vacuum furnace, and poured it through a narrow tube to remove oxide and dross, which adhered to the walls of the tube. From this material, we grew single crystals in soot-coated Pyrex crucibles by cooling from the melt in the temperature gradient at the end of a horizontal furnace. We oriented the crystals using a reflected laser beam and Laue back scattering of X-rays.

We cut parallel-sided slabs a few millimeters thick from the crystals, using a Servomet spark cutter. The faces of each slab were perpendicular to a selected crystallographic axis to within ± 1°. The residual resistivity ratio $R_{300K}/R_{4.2K}$ of the specimens after cutting was typically 400. One face of each slab was chemically polished. We painted two insulating strips onto this surface, to insulate the two superconducting connecting strips (one connecting the teeth of each comb) from the bismuth. We exposed the crystal to an argon glow discharge in an evaporator to remove most of the surface contamination, pumped out the argon, and evaporated the tin teeth of the combs through a mask onto the cleaned surface. The mask consisted of ten slits (5 per comb) 50μm wide and 100μm apart cut into a copper foil using a photolithographic technique. For each comb, the ends of the teeth nearer the edge of the crystal overlapped one of the insulating strips. These ends were subsequently connected together by tin cross-strips evaporated through masks onto the insulating layers.

For some of the samples, we evaporated only a single tooth for each comb. In this case, the teeth were typically 10μm wide. In preparing one of the earlier specimens (3-1), we cleaved the slab from the bismuth crystal, quickly painted on the insulating layer, and

evaporated the tin without further cleaning. This method appeared to produce sufficiently clean surfaces. However, the cleaving apparently introduced damage near the surface that significantly reduced the mean free path, and this method was not used subsequently.

2.3 Apparatus

The resistance R(H) of each sample, typically $10^{-5}\Omega$, was determined using a null-balancing technique. A superconducting galvanometer[6] (SLUG) in series with a known resistance R_s was connected across the two combs. The output from the galvanometer was amplified, and the amplified voltage fed via a large resistance into R_s to maintain zero current in the galvanometer. A constant current, typically 1mA per pair of teeth, was passed between the two combs, and the appropriate null-balancing current established in R_s. The magnetic field H was slowly swept, and the change in the feedback current, which was proportional to $\Delta R(H) = R(H) - R(0)$, plotted vs H on an X-Y recorder. The resolution was approximately $10^{-9}\ \Omega$. When the field was changed, there was a very large induced voltage in the measuring circuit. The field was therefore changed in small steps, and the transient currents allowed to decay before each datum point was recorded.

The specimen, galvanometer, R_s, and field solenoid were immersed in liquid helium. The temperature of the bath was regulated using a bridge circuit designed by Rochlin.[7] Electrical contact to the superconducting cross strips on the sample was made with strips of lead pressed down lightly with springs. The teeth were aligned with the magnetic field to within ± 2°. The galvanometer was situated about 20 cm from the sample, and enclosed in a superconducting box. The

ambient field was reduced to a few mG by surrounding the cryostat with two concentric mu-metal cylinders. The superconducting solenoid used to generate the magnetic field was calibrated to an accuracy of ± 2%.

We attempted to measure the derivative dR(H)/dH by superimposing a small low frequency alternating current on the solenoid current, and measuring the amplitude of the alternating current fed back into R_s. Unfortunately, the inductive signal in the voltmeter leads was several orders of magnitude larger than the signal developed across the sample. Our efforts to reduce this spurious signal to a manageable level by means of a bucking coil were not successful.

3. THE FERMI SURFACE OF BISMUTH

Bismuth is a group V semimetal with a rhombohedral lattice that is only slightly distorted from simple cubic. The crystallographic axes are a right-hand triad in which the trigonal (z) axis is the axis of 3-fold symmetry, the binary (x) axis is one of three axes of 2-fold symmetry, and the bisectrix (y) axis is perpendicular to the x- and z-axes. The semimetallic nature of bismuth arises from the small overlap in energy between the fifth and sixth Brillouin zones, which results in a small number of electrons ($\sim 10^{-5}$ per atom) and an equal number of holes.

The Fermi surface of bismuth has been extensively investigated both experimentally and theoretically,[8] and its parameters are very well known. The electron Fermi surface consists of three highly elongated prolate ellipsoids. The non-parabolic energy-momentum

relation for ellipsoid I is[9]

$$E_e(1+E_e/E_g) = E_e' = (\hbar^2/2m_o)(\alpha_{xx}k_x^2+\alpha_{yy}k_y^2+\alpha_{zz}k_z^2+2\alpha_{yz}k_yk_z). \quad (2)$$

Here, m_o is the free electron mass, α_{ij} is a component of the electron inverse effective mass tensor, E_e is the electron Fermi energy measured from the bottom of the conduction band, and E_g is the energy gap. Ellipsoids II and III are obtained by rotations of $2\pi/3$ about the trigonal axis. The cross term in k_y and k_z arises because the principal axes of the ellipsoids are tilted with respect to the crystallographic axes by an angle of approximately 6° about the binary axis.

The Fermi surface of the holes is a prolate ellipsoid of revolution described by the parabolic dispersion relation[8]

$$E_h = (\hbar^2/2m_o)[\beta_1(k_x^2+k_y^2) + \beta_3k_z^2]. \quad (3)$$

Here, β_i is a component of the hole inverse effective mass tensor, and E_h is the Fermi energy for the holes measured from the top of the valence band.

Figure 2 is a schematic view (not to scale) along the trigonal axis in the extended zone scheme.

4. RESULTS

We obtained data from six specimens, for three different crystal orientations, and for configurations with five teeth per comb and a single tooth per comb. The variation of R(H) with H for representative

samples is shown in Figs. 3-7. Each plot exhibits at least one minimum or shoulder in R(H), corresponding to a Fermi surface extremal diameter. The results are therefore in qualitative agreement with Pippard's predictions.[1] In each case, the minimum in R(H) is superimposed on a background resistance that increases with H: this rise is due to the magnetoresistance of the bismuth. Particularly in Figs. 3 and 4, the minimum at H_m and the rising background combine to produce a pronounced maximum near $H_m/2$.

For an ellipsoid, the extremal diameter and the diameter are the same in any direction. The important experimental parameters and the values of D_{xe} and D_{ze} deduced from the data are summarized in Table I. The diameters of an electron ellipsoid along its principal axes are referred to as D_{1e}, D_{2e}, and D_{3e}. The diameters of an electron ellipsoid along the crystallographic axes are D_{xe}, D_{ye}, and D_{ze}, where $D_{1e} = D_{xe}$. The diameters of the hole ellipsoid of revolution are D_{1h}, D_{2h}, and D_{3h}, where $D_{1h} = D_{2h}$.

4.1 Trigonal Plane

The tin strips were evaporated onto the trigonal (x - y) plane, and the magnetic field was also in the trigonal plane. The diameters measured are D_{ze} for all three electron ellipsoids, and D_{3h} for the hole ellipsoid, regardless of the direction of the field relative to the x and y axes. D_{3h} is roughly seven times D_{ze}.

We obtained data from two samples, 3-1 and 3-2, each having two interlocking combs of five teeth (see Table I). The surface of sample 3-1 was produced by cleaving. For both samples, R(H) exhibited a minimum corresponding to D_{ze}. R(H) vs H for 3-2 is shown in Fig. 3. H_m is the field at which the minimum occurs. For comparison, we have

calculated H_o from the magneto-acoustic attentuation work of Korolyuk,[10] using Eq. (1) (see section 5.2). There is some evidence of points of inflection near $H_m/3$ and $H_m/5$, corresponding to electron focusing between more distant teeth of the two combs. For sample 3-2, H was swept up to 100G,but no structure corresponding to D_{3h} was observed.

4.2 Binary Plane

The tin strips were evaporated onto the binary (y-z) plane, and the magnetic field was applied in the y-z plane. We see from Fig. 2 that there are three distinct diameters along the x-axis. In order of increasing size and regardless of the orientation of the field in the y-z plane, the three diameters measured are: the diameter of ellipsoid I, D_{1e}; the diameter of ellipsoids II and III (along the x-axis); and the diameter of the hole ellipsoid, D_{1h}.

We obtained data for three samples (see Table I). Specimen 2-1 had the comb configuration, while 2-2 was made from 2-1 by scribing through all the teeth on each comb except one. R(H) for these samples is shown in Figs. 4 and 5. Each curve exhibits a minimum at H_m corresponding to D_{xe} but no structure corresponding to the two larger diameters. Again, for comparison, we have indicated the values of H_{oe1} (corresponding to D_{xe}), H_{oe2} (corresponding to the diameter of ellipsoids II and III), and H_{oh} (corresponding to D_{1h}) calculated from Korolyuk's data.[10]

In sample 2-3, there was a single tooth on each comb. The two teeth were of unequal width being respectively 8μ and 4μ. R(H) for this specimen appears in Fig. 6. In addition to the minimum corresponding to D_{xe}, there is a shoulder associated with the diameter of ellipsoids II and III.

R(H) was an even function of H for all samples except 2-3. For this sample, R(H) was asymmetric with respect to the direction of H, as indicated in Fig. 6. However, R(H) was symmetric in H if the polarity of the specimen current I was reversed when H was reversed. R(H) was unaffected by doubling the value of I, indicating that the asymmetry in R(H) was not due to the self-field of the current. The asymmetry was in fact a result of the different strip widths, which produced an asymmetric current distribution. Consider the current distribution along an axis y that lies on the crystal surface and intersects the two teeth at right angles. The origin is midway between the teeth. If the current distribution is uniform across each strip and the strip widths are equal, the current distribution is an odd function of y. When the current distribution is an odd function of y, the voltage between two points y_o and $-y_o$ at the surface is an even function of H.[11] Thus, if the strips are equal in width, R(H) will be even in H. However, if the strips are unequal in width, the symmetry in the current distribution is lost, and in general R(H) will not be an even function of H.

4.3 Bisectrix Plane

The combs were evaporated onto the bisectrix (x-z) plane and the magnetic field was in the x-z plane. The three diameters measured, in order of increasing size and regardless of the orientation of the field in the x-z plane are: the diameter of the ellipsoids II and III along the y axis; the diameter of the hole ellipsoid D_{2h} (= D_{1h}); and the diameter D_{ye} of ellipsoid I. We obtained data for one specimen, 1-1, with a single tooth on each comb and the field parallel to the z-axis (Table I). R(H) is shown in Fig. 7. The values of H_{oel} and H_{oh} have been calculated

from Korolyuk's data.[10] R(H) has no distinct minima, but exhibits two shoulders corresponding to the diameter of ellipsoids II and III, and to D_{1h}.

4.4 Temperature Dependence

The temperature dependences of several quantities over the range 1.4K to 3.7K for sample 3-2 are exhibited in Fig. 8. Figure 8(a) shows the temperature dependence of H_m. Figure 8(b) shows the temperature dependence of the amplitude of the minimum, defined as the difference between $R(H_m)$ and the maximum value of R(H) for $H < H_m$. Figure 8(c) shows R(0) as a function of temperature.

5. ANALYSIS OF RESULTS

In this section, we make a detailed comparison of our results with the theory of Gonçalves da Silva. We also compare our values of Fermi surface diameters with those in the literature.

5.1 Mean Free Path Effects

Printer: $\mathcal{C}$ script cee

For circular orbits, we expect to observe focusing effects only if $\omega_c\tau \gtrsim 1$, or equivalently $\ell/d \gtrsim 1/2$. For non-circular orbits, this condition may be generalized to $2\pi\ell/\mathcal{C} \gtrsim 1$, where $\mathcal{C}$ is the orbit circumference. It is difficult to accurately determine the mean free path of our samples because of the high degree of anisotropy of bismuth. However, Hartman[12] in his work on the low-field galvanomagnetic coefficients has determined the relaxation-time tensor $\bar{\bar{\tau}}$ for the electrons and holes at 4.2K in bismuth crystals with a residual resistivity ratio of about 400. From $\bar{\bar{\tau}}$ he calculates the following mean free paths along the ellipsoid axes:

$$\ell_{1e} = 390\mu m, \quad \ell_{2e} = 120\mu m, \quad \ell_{3e} = 300\mu m,$$
$$\ell_{1h} = \ell_{2h} = 230\mu m, \quad \ell_{3h} = 110\mu m. \tag{4}$$

If we assume these values of mean free paths, we find $\ell/d \sim 1$ for all specimens in which the orbits were nearly circular. The only specimen for which the orbits were highly non-circular was 1-1, where the tin strips were oriented parallel to the trigonal axis on the bisectrix surface. For this specimen electrons from ellipsoids II and III (the smallest diameter) had highly elongated trajectories. The ratio of the trajectory length to d was about 18, and $2\pi\ell/\mathcal{C} \ll 1$. Thus the minimum (at H_{oe1} in Fig. 7) was smeared out into a barely perceptible shoulder.

5.2 The Role of w/d

The parameter w/d plays an important role in the theory of Gonçalves da Silva. He shows that in general H_m, the value of field at which the minimum occurs, is less than H_o, the value of field for which the diameter of the trajectory in real space is d. H_m and H_o coincide only in the limit $w/d \to 0$. Thus, the Fermi surface diameter D must be obtained from H_m using Eq. (1) and the value of the ratio H_m/H_o, which is a function of w/d. The solid curve in Fig. 9 is H_m/H_o versus w/d according to the model of Gonçalves da Silva, and the points are from our experimental results. Since we measure only H_m, we have used values of H_o calculated from Korolyuk's data[10] to calculate H_m/H_o. The error bars include the estimated errors in our own measurements and in those of Korolyuk. The values of H_m/H_o for

three binary samples are independent of w/d to within the experimental error. Evidently, H_m/H_o for these samples does not decrease with increasing w/d as predicted by the theory. It also appears that the value of H_m/H_o for the lowest value of w/d is significantly less than unity.

However, other aspects of the data are well explained by the theory. The existence of structure in R(H) associated with Fermi surface diameters other than the smallest also depends strongly on w/d in the theoretical model. For example, the structure arising from the hole sphere, which has the largest diameter, is smeared out for large w/d. As w/d is reduced, a shoulder associated with the hole orbits appears, as is seen in Fig. 3 of the following paper. Our experimental results are consistent with this result. For the samples 3-1, 3-2, and 2-1 with the larger values of w/d, the only minimum in R(H) is that corresponding to the smallest Fermi surface diameter. For samples 1-1 and 2-3, which have smaller values of w/d, there is also a shoulder associated with the second smallest diameter. The model predicts the appearance of this shoulder in the range $0.10 < w/d < 0.25$; experimentally the shoulder appears in the range $0.12 < w/d < 0.17$. The model also predicts that the second shoulder should occur at a magnetic field appreciably less than H_o, even for relatively small values of w/d. If we gauge the position of the shoulder at the point of maximum curvature in the plot of R(H) versus H, we find from Fig. 3 of the paper by Gonçalves da Silva that the shoulder corresponding to the hole surface occurs at about 0.88 H_o. For sample 2-3, the shoulder corresponding to the hole surface occurs at 0.78 H_o.

The model is very successful in describing the general shape of the structure observed experimentally. It also accounts successfully for the appearance of additional structure as the value of w/d is lowered. The only major failure of the model is in its prediction of the dependence of H_m/H_o on w/d. It is not entirely clear which aspect of the model is responsible for this failure. The model assumes a Fermi surface consisting of three electron spheres and one hole sphere; although topologically equivalent, the ellipsoids of the bismuth Fermi surface depart considerably from spheres. The model also assumes that $\omega_c\tau \gg 1$ whereas in our experiment $\omega_c\tau \sim 1$. However, neither of these approximations seems likely to affect the dependence of H_m/H_o on w/d appreciably.

A more serious difficulty concerns the manner in which the current enters and leaves the bismuth surface. First, the model assumes that the current flows uniformly along the superconducting strips, and is injected uniformly into the sample. In practice, the current flows preferentially along the edges of the superconducting strips,[13] and is injected non-uniformly into the bismuth. This non-uniform current distribution could well produce an experimental dependence of H_m/H_o on w/d that differs significantly from that predicted by the model. Second, the model requires a thin resistive layer on the surface of the crystal. This layer allows the potential to vary along the surface of the crystal under the superconducting strips. In our samples, the resistance of this layer was rather small. For example, the measured resistance of sample 3-2 was only 30% above the value we estimated assuming zero surface resistance. We know from subsidiary experiments that the argon

glow discharge was fairly effective in removing the surface oxide layer from the bismuth sample, although the bombardment of the surface undoubtedly introduced some lattice disorder. It seems likely that the resistive layer was not sufficiently thick to allow the potential to vary across the surface under the superconducting strips as demanded by the model. Rather, the potential was probably almost constant.

It seems most likely that either the non-uniform current injection or the lack of a resistive surface layer is responsible for the observed lack of dependence of H_m/H_o on w/d. The current injection could presumably be made uniform by evaporating an insulating layer and then a superconducting ground plane over the combs. The requirement of a resistive surface layer is more difficult to meet. If a high resistance is introduced, it will be much more difficult to observe the resistance minima, whose amplitude will be unchanged. It may therefore always be difficult to obtain accurate Fermi surface data from samples with high w/d.

5.3 Temperature Dependence

The temperature dependences of several quantities for sample 3-2 appear in Fig. 8. The value of H_m is independent of temperature as we expect, since H_m depends only on the Fermi surface diameter. The amplitude of the minimum is also independent of temperature. This result is also expected: the amplitude depends on the bulk resistivity of the bismuth which is impurity- and defect-limited and is therefore independent of temperature in this temperature range.

Figure 8(c) shows that R(0) increases rapidly as the temperature is increased towards the tin transition temperature, T_c. This behavior

is similar to that observed by Pippard, Shepherd, and Tindall[14] in their work on the temperature dependence of the resistance of the superconductor-normal metal interface. At temperatures well below T_c, the energies of almost all quasiparticles incident on the interface from the normal metal lie below the superconducting energy gap, $\Delta(T)$. These quasiparticles suffer Andreev[15] reflection. In this process, a quasiparticle above (below) the Fermi level is scattered into one below (above) with the same energy. At the same time, a pair is created in the superconductor. Consequently, the normal current in the bismuth is converted into a supercurrent in the tin at the interface. As the temperature is increased, the quasiparticle energies rise, and $\Delta(T)$ falls. Quasiparticles with energies greater than $\Delta(T)$ have a non-zero probability of being transmitted into the tin, where they constitute a dissipative quasiparticle current. This current decays in a characteristic time[16] τ_Q over a characteristic length[14] $\lambda_Q = (\ell_S v_F \tau_Q/3)^{1/2}$, assuming that the mean free path in the tin, ℓ_S, is much less than λ_Q. The dissipation is manifested as additional resistance. As the temperature increases, more quasiparticles penetrate into the superconductor, and the resistance increases.

As the temperature is raised towards T_c, the position and amplitude of the minimum remain fixed, although R(0) increases dramatically, demonstrating that the minimum arises from a bulk effect rather than from a surface effect.

5.4 Substructure

With the tin strips in the comb configuration, one expects to observe additional minima in R(H) at $H_m/3$, $H_m/5$, etc., arising from focusing between more distant teeth of the two combs. Specimen 3-2 was

the only sample for which these minima were observed. The minima near $H_m/3$ and $H_m/5$ are much smaller in amplitude than the minimum at H_m, since $\omega_c\tau$ was rather less than unity for these relatively long trajectories. The minima do not occur at exactly $H_m/3$ or $H_m/5$, for reasons that are not clear in the absence of any detailed theory for this configuration.

5.5 Comparison With Other Fermi Surface Data

Table I summarizes the values of D_{xe} and D_{ze} deduced from our data. In the absence of any reliable information on the exact value of H_m/H_o, we have simply assumed that $H_m = H_o$, and $D = eH_m d/\hbar c$. It is clear from Fig. 9 that there is no evidence for a dependence of H_m/H_o on w/d, as expected from the theoretical model. We also observe that H_m lies somewhat below Korolyuk's value[10] for H_o. We therefore expect our diameters to be somewhat smaller than those quoted in the literature. It is likely that our values should be systematically increased to account for discrepancies arising from the rather large values of w/d used in many of our samples. This possible systematic error has not been included in our error estimates. The quoted errors include our estimated errors in the magnetic calibration (a systematic error), the strip separation, the crystal alignment, and the determination of H_m from R(H) versus H. The average values of the diameters are $D_{xe} = (0.94 \pm 0.03) \times 10^{-2}$ Å^{-1} and $D_{ze} = (1.35 \pm 0.04) \times 10^{-2}$ Å^{-1}.

The electronic structure of bismuth has been extensively studied. However, one must exercise care in the calculation of diameters from certain types of Fermi surface measurements as there is still uncertainty in some of the band structure parameters. For example, Dresselhaus[17] has pointed out that the value of $E_g = 0.015$ eV obtained by Brown,

Mavroides, and Lax[18] has been widely accepted, although a more recent measurement by Maltz and Dresselhaus[19] yields $E_g = 0.011$ eV. One should preferably estimate diameters from results of other size effect measurements or from de Haas-van Alphen experiments, which do not require a knowledge of the band structure for the calculation (as is the case for cyclotron resonance, for example).

In Table II, we compare our diameters D_{xe} and D_{ze} with those obtained from other size effect experiments and from the very careful and complete de Haas-van Alphen work of Bhargava.[20] Although inversion theorems exist for calculating diameters from the extremal cross-sectional areas obtained from a de Haas-van Alphen experiment,[21,22] we have not used them since the Fermi surface is known to be made up of ellipsoids. We have calculated diameters from Bhargava's results[20] using the result for an ellipsoid:

$$D_1 = \frac{2}{\sqrt{\pi}} \left(\frac{A_2 A_3}{A_1} \right)^{1/2}, \tag{5}$$

and analogous expressions for D_2 and D_3. D_i is a diameter along a principal axis of the ellipsoid, and A_i is the area of the extremal section normal to that axis. For comparison with our results, the diameters along the crystallographic axes were calculated using the expressions

$$D_x = D_1,$$

and

$$D_z = (D_3^{-2} \cos^2\theta_t + D_2^{-2} \sin^2\theta_t)^{-1/2}. \tag{6}$$

Here, θ_t is the angle of tilt of the ellipsoid along the binary axis, about 6°. Our diameters lie consistently below those of other workers, although the agreement is generally just within the experimental errors. As explained above, it is likely that our diameters should be systematically increased, probably by a few percent, to account for the fact that H_m may lie below H_o. However, a detailed study of the dependence of H_m/H_o on w/d would be necessary in order to estimate such a correction.

6. SUMMARY

We have observed local minima in the resistance between two superconducting combs or superconducting strips on the surface of a bismuth crystal as a function of magnetic field. The minima arise from the focusing of electrons or holes. This observation confirms the prediction of Pippard.[1]

The experimental results using one pair of superconducting strips are in good qualitative agreement with several of the predictions of the model of Gonçalves da Silva.[2] The general shapes of the observed R(H) versus H curves are very similar to those of the model. In particular, R(H) exhibits a minimum corresponding to the smallest extremal Fermi surface diameter for a variety of values of w/d. As w/d is reduced in value, R(H) develops a shoulder corresponding to the second smallest diameter. However, as w/d is increased from zero, the observed value of H_m/H_o does not decrease from unity as predicted by the model. It is likely that this discrepancy arises from one of two differences between the model and the experiment: First, the model assumes a uniform current flow along the superconducting strips, whereas in our

experiment, the current density was undoubtedly higher near the edges of the strips. Second, the model assumed a resistive layer between the strips and the crystal, whereas in our experiment the strips were in relatively good electrical contact with the crystal. The first difficulty could probably be overcome experimentally with the use of a superconducting ground plane (which might, however, distort the magnetic field somewhat). The second difficulty should be tackled both experimentally and theoretically. It would be of some interest to calculate R(H) using a model in which the potential at the surface is held constant across the superconducting strips.

We have estimated values for the diameters D_{xe} and D_{ze} of the principal electron ellipsoid, and find $D_{xe} = (0.94 \pm 0.03) \times 10^{-2}$ Å^{-1} and $D_{ze} = (1.35 \pm 0.04) \times 10^{-2}$ Å^{-1}. These values lie somewhat below those in the literature, but are just within the combined experimental errors. It is likely that this discrepancy arises because H_m/H_o is somewhat less than unity, whereas we have assumed $H_m = H_o$.

This technique has the potential of being a useful one for the accurate determination of extremal Fermi surface diameters. It would clearly be necessary to resolve the discrepancy between experiment and theory in the dependence of H_m/H_o on w/d. It would probably be advantageous to use values of w/d of about 10^{-2}. It would be helpful to measure dR(H)/dH: The derivative would probably reveal structure in R(H) that we were unable to observe and enable the positions of the minima to be more accurately located. Finally, it would be most interesting to look for the focusing effect in a metal, for example copper.

7. ACKNOWLEDGEMENTS

We are pleased to acknowledge many helpful discussions with Dr. Cylon Gonçalves da Silva.

This work was supported by the U. S. Atomic Energy Commission.

Table I

Summary of Experimental Results

Specimen	Orientation	Pairs of Teeth	w/d^a	d^a (μm)	H_m (G)	Diameter ($10^{-2}Å^{-1}$)
3-1	trigonal	5	0.56	98±1	9.05±.36	D_{ze}=1.35±.06
3-2	trigonal	5	0.54	99±1	8.95±.14	D_{ze}=1.35±.04
2-1	binary	5	0.54	101±2	6.00±.07	D_{xe}=0.92±.03
2-2	binary	1	0.17	295±3	2.17±.07	D_{xe}=0.97±.04
2-3	binary	1	0.035	171±3	3.55±.07	D_{xe}=0.92±.03
1-1	bisectrix	1	0.12	206±3	-	-

[a] w/d and d have been averaged where applicable.

Table II

Comparison of Diameters

Investigator	Method	Diameter ($10^{-2}Å^{-1}$) D_{xe}	D_{ze}
Bhargava[20]	de Haas-van Alphen	1.05±.04	1.39±.05
Korolyuk[10]	magneto-acoustic effect	1.04±.04	1.45±.06
Reneker[23]	magneto-acoustic effect	1.02±.05	1.48±.07
Khaikin and Edelman[24]	cylotron-resonance cut-off	1.02±.03	-
Herrmann *et al.*[25]	rf size effect	1.03±.02	-
Present work	focusing	0.94±.03	1.35±.04

REFERENCES

1. F. M. Hawkins and A. B. Pippard, Proc. Camb. Phil. Soc. 61, 433 (1965).
2. C. Gonçalves da Silva, following paper.
3. M. S. Khaikin, Zh. Eksperim.i.Teor. Fiz. 41, 1773 (1961) [English transl: Sov. Phys.JETP 14, 1260 (1962)].
4. See V. F. Gantmakher, in Progress in Low-Temperature Physics, Vol. 5, p. 181, edited by C. J. Gorter (North-Holland, Amsterdam, 1966).
5. See A. R. Mackintosh, in Phonons and Phonon Interactions, p. 181, edited by T. A. Bak (W. A. Benjamin, Inc., New York, 1964).
6. J. Clarke, Phil. Mag. 13, 115 (1966).
7. G. I. Rochlin, Rev. Sci. Inst. 41, 73 (1970).
8. For recent references, see the review article by M. S. Dresselhaus, in Physics of Semimetals and Narrow-Gap Semiconductors, edited by D. L. Carter and R. T. Bate (Pergamon, New York, 1971), or the review article by A. P. Cracknell, Adv. Phys. 18,681 (1969); for references to the literature before 1961, see the review article by W. S. Boyle and G. E. Smith, in Progress in Semiconductors, vol. 7, edited by A. F. Gibson and R. E. Burgess (Wiley, New York, 1963).

9. In this paper we assume the Lax ellipsoidal non-parabolic model for the electron Fermi surface (B. Lax, J. G. Mavroides, H. J. Zeiger, and R. J. Keyes, Phys. Rev. Letters 5, 241 (1960)). Recent experiments (R. J. Dinger and A. W. Lawson, Phys. Rev. B7, 5215 (1973), and R. Herrmann, S. Hess, and H.-U. Müller, Phys. Status Solidi B48, K151 (1971)) suggest that the electron Fermi surface may deviate somewhat from ellipsoidal, as suggested by Cohen (M. H. Cohen, Phys. Rev. 121, 387 (1961)).

10. A. P. Korolyuk, Zh. Eksperim. i Teor. Fiz. 49, 1009 (1965) [English Transl: Sov. Phys. JETP 22, 701 (1966)].

11. C. Gonçalves da Silva, private communication.

12. R. Hartman, Phys. Rev. 181, 1070 (1969).

13. V. L. Newhouse, J. W. Bremer and H. H. Edwards, Proc. IRE 48, 1395 (1960).

14. A. B. Pippard, J. G. Shepherd, and D. A. Tindall, Proc. Roy. Soc. London A324, 17 (1971).

15. A. F. Andreev, Zh. Eksperim i. Teor. Fiz. 46, 1823 (1964) [English transl: Sov. Phys. JETP 19, 1228 (1964)].

16. J. Clarke, Phys. Rev. Letters 28, 1363 (1972); M. Tinkham and J. Clarke, Phys. Rev. Letters 28, 1366 (1972); M. Tinkham, Phys. Rev. B6, 1747 (1972); J. Clarke and J. L. Paterson, to be published in Jour. Low Temp. Phys.

17. M. S. Dresselhaus, loc. cit.

18. R. N. Brown, J. G. Mavroides, and B. Lax, Phys. Rev. 129, 2055 (1963).

19. M. Maltz and M. S. Dresselhaus, Phys. Rev. B2, 2877 (1970).

20. R. N. Bhargava, Phys. Rev. 156, 785 (1967).

21. I. M. Lifshitz and A. V. Pogorelov, Dokl. Akad. Nauk SSR 96, 1143 (1954).

22. F. M. Mueller, Phys. Rev. 148, 636 (1966).

23. D. H. Reneker, Phys. Rev. 115, 303 (1959).

24. M. S. Khaikin and V. S. Edelman, Zh. Eksperim i. Teor. Fiz. 47, 878 (1964) [English transl:Sov. Phys. JETP 20, 587 (1965)].

25. R. Herrmann, S. Hess, and H.-U. Müller, Phys. Stat. Sol. B 48, K151 (1971).

Figure Captions

Fig. 1. Experimental geometry: (a) Plan view. (b) Side view, showing electron trajectories for three values of magnetic field H.

Fig. 2. Schematic view (not to scale) along the z-axis of the Fermi surface of bismuth in the extended zone scheme.

Fig. 3. R(H) versus H for sample 3-2.

Fig. 4. R(H) versus H for sample 2-1.

Fig. 5. R(H) versus H for sample 2-2.

Fig. 6. R(H) versus H for sample 2-3: the direction of H is reversed in the upper figure relative to the direction in the lower figure. The insert in the lower figure is expanded plot near H_m.

Fig. 7. R(H) versus H for sample 1-1.

Fig. 8. Temperature dependence of (a) H_m, (b) amplitude of minimum, and (c) R(0) for sample 3-2.

Fig. 9. Experimental (data points) and theoretical (curve) dependence of H_m/H_o on w/d. The values H_o for the experimental points have been calculated from the work of Korolyuk.[10]

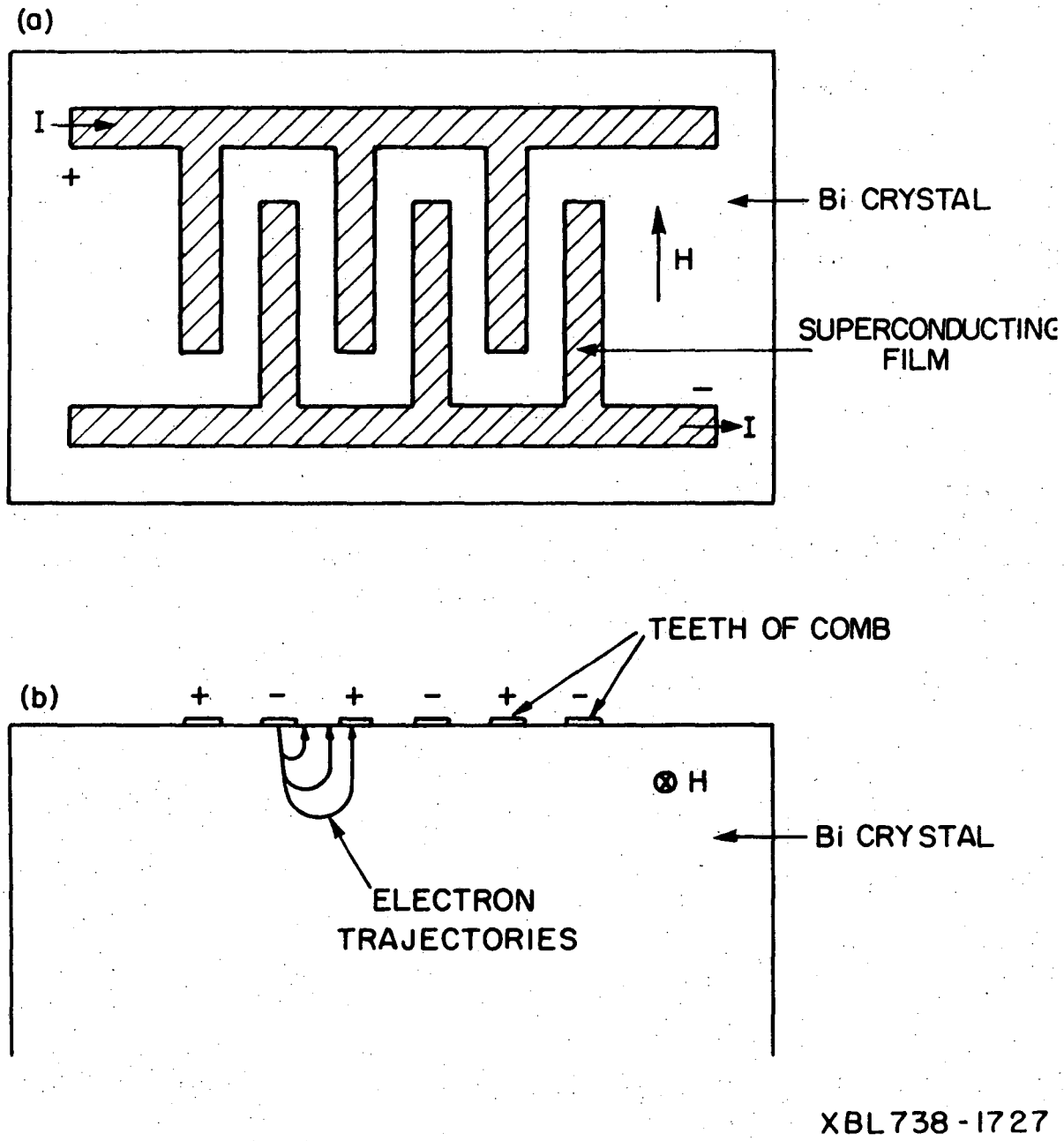
(a)
I
+
Bi CRYSTAL
H
SUPERCONDUCTING
FILM
−
I
TEETH OF COMB
(b)
+
−
+
−
+
−
⊗ H
Bi CRYSTAL
ELECTRON
TRAJECTORIES
XBL738-1727

Fig. 1

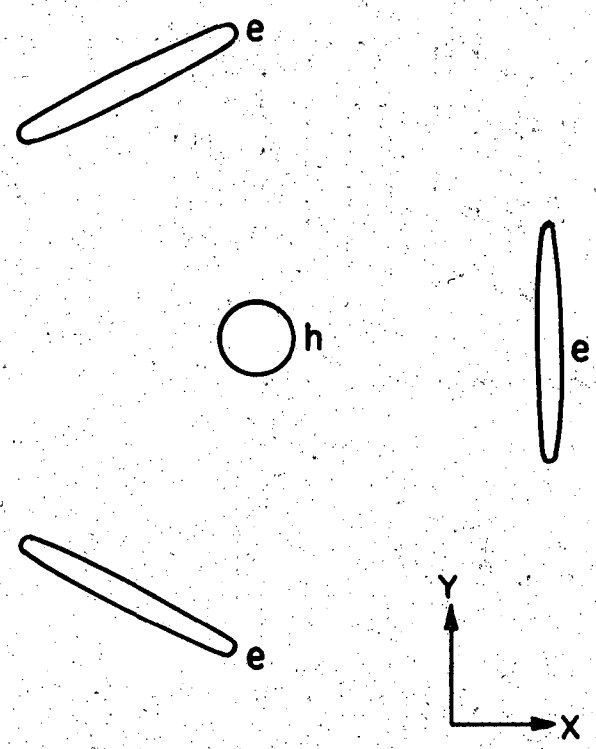

e ELECTRONS

h HOLES

XBL 738-1724

Fig. 2

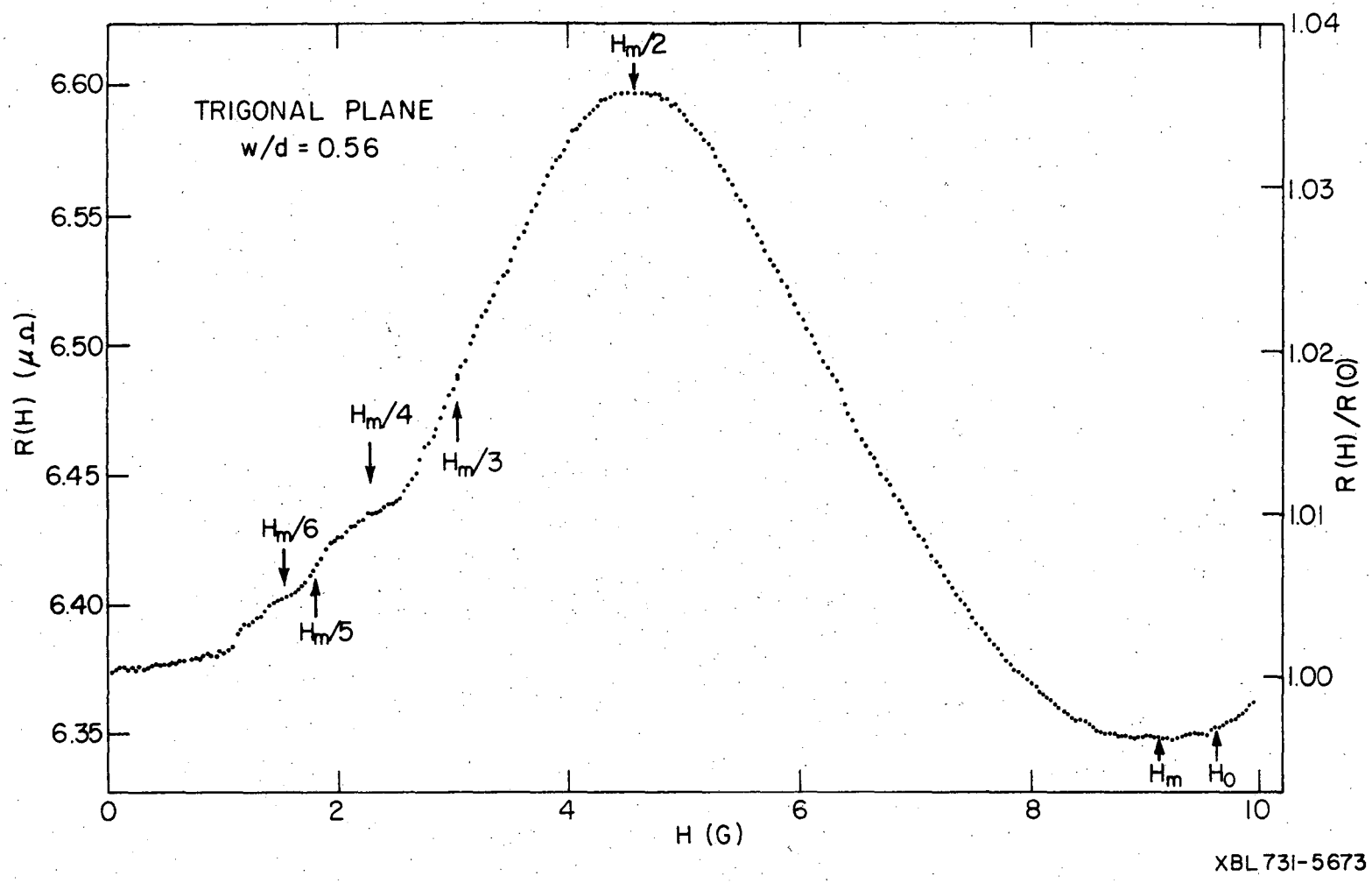
TRIGONAL PLANE
w/d = 0.56
R(H) (μΩ)
R(H)/R(0)
H (G)
Hm/2
Hm/4
Hm/3
Hm/6
Hm/5
Hm
H0
6.60
6.55
6.50
6.45
6.40
6.35
1.04
1.03
1.02
1.01
1.00
0
2
4
6
8
10
XBL 731-5673

Fig. 3

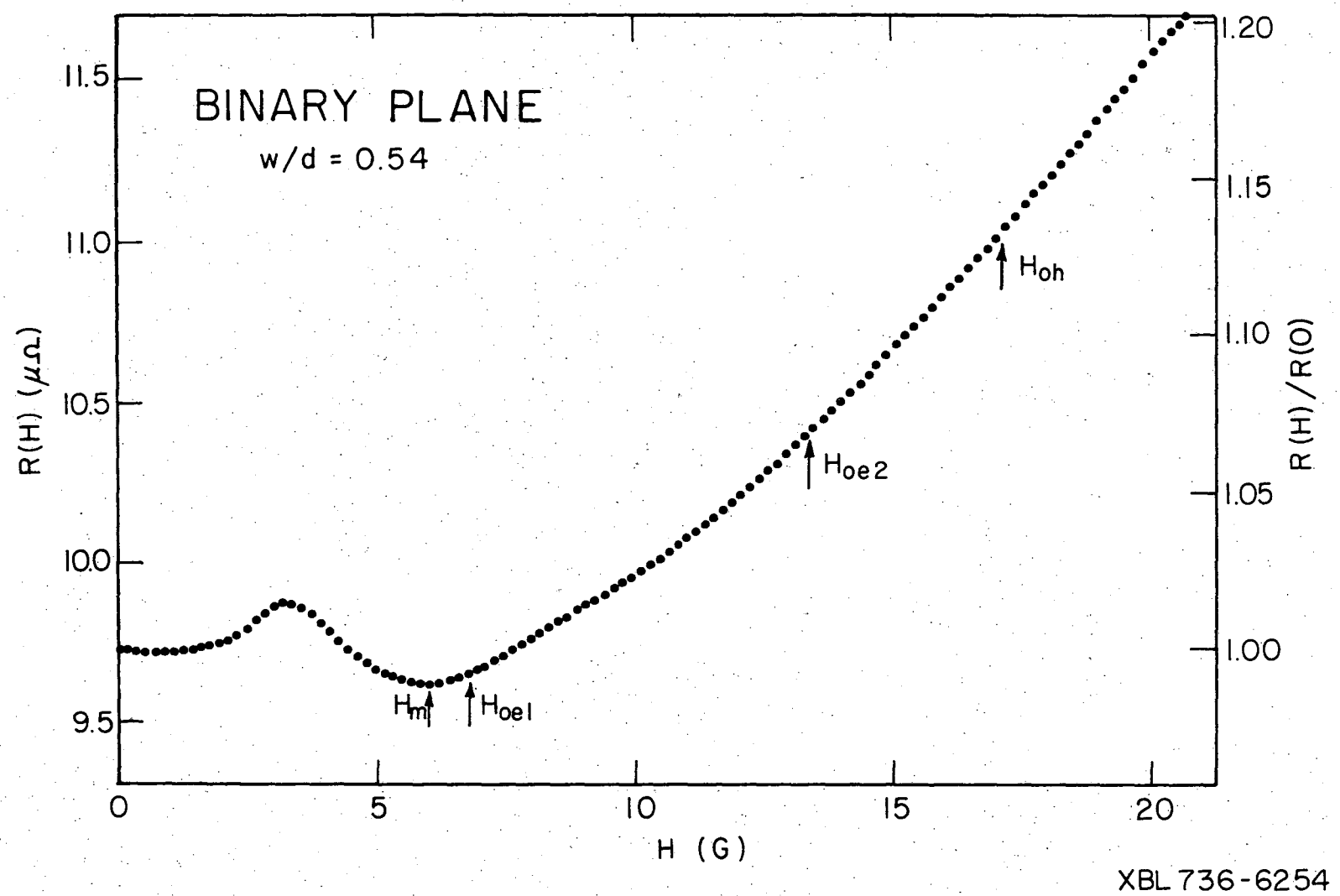
BINARY PLANE
w/d = 0.54
R(H) (μΩ)
R(H)/R(0)
H (G)
11.5
11.0
10.5
10.0
9.5
1.20
1.15
1.10
1.05
1.00
0
5
10
15
20
Hm
Hoe1
Hoe2
Hoh
XBL 736-6254

Fig. 4

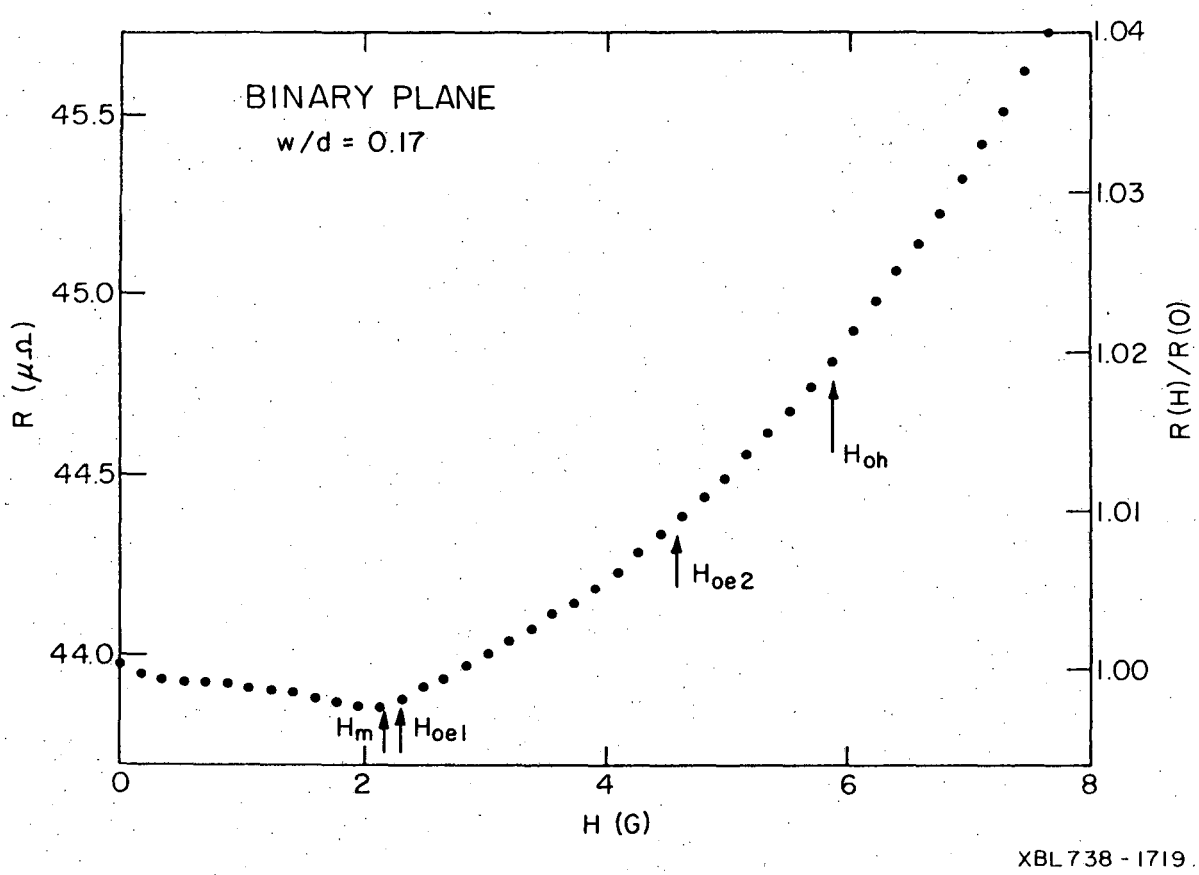
BINARY PLANE
w/d = 0.17
45.5
45.0
44.5
44.0
R (μΩ)
1.04
1.03
1.02
1.01
1.00
R(H)/R(0)
Hoh
Hoe2
Hm
Hoe1
0
2
4
6
8
H (G)
XBL 738 - 1719

Fig. 5

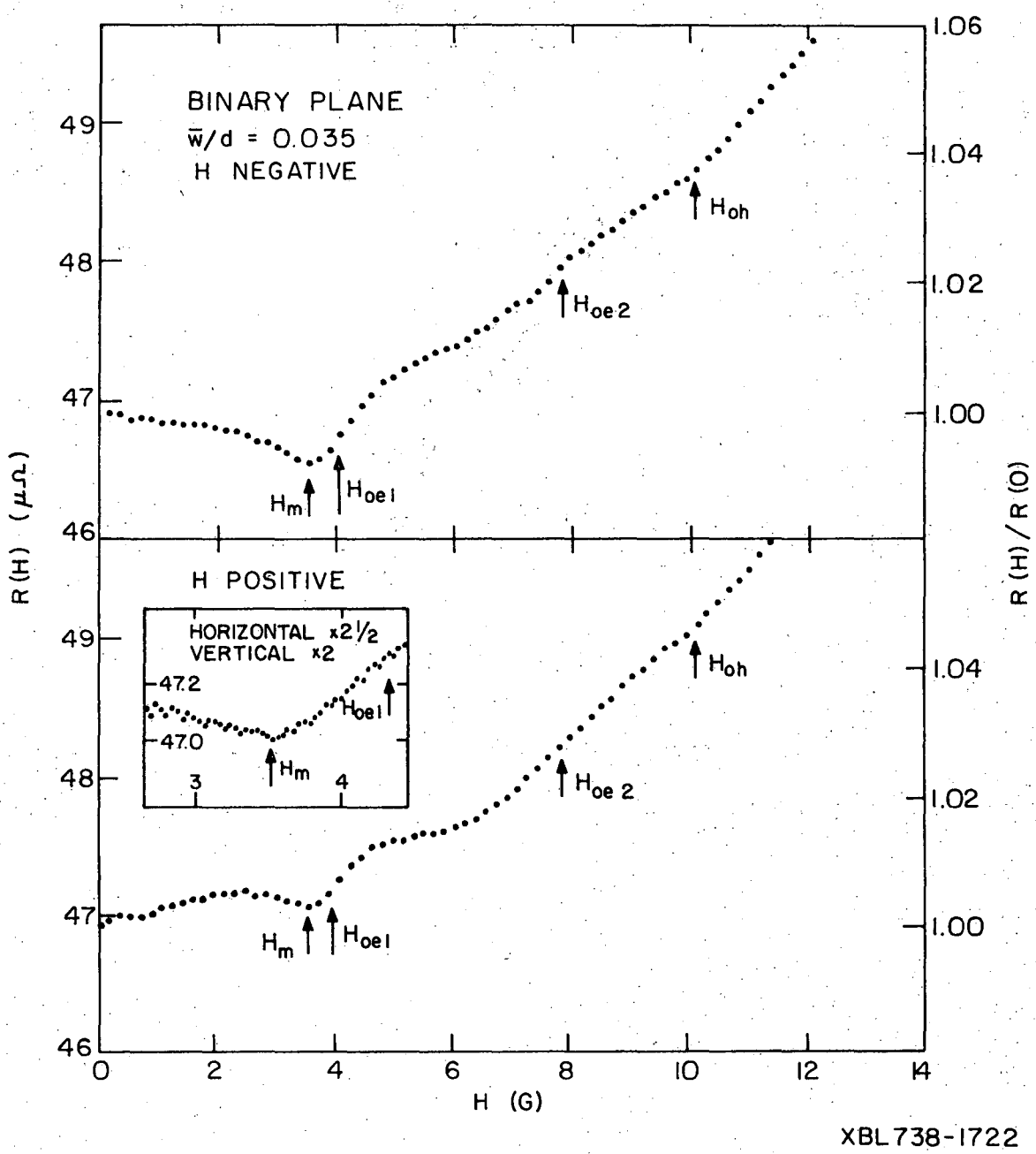
BINARY PLANE
w̄/d = 0.035
H NEGATIVE
H POSITIVE
HORIZONTAL x2½
VERTICAL x2
47.2
47.0
3
4
Hm
Hoe1
Hoe2
Hoh
R (H) (μΩ)
R (H)/R (0)
H (G)
46
47
48
49
1.00
1.02
1.04
1.06
0
2
4
6
8
10
12
14
XBL738-1722

Fig. 6

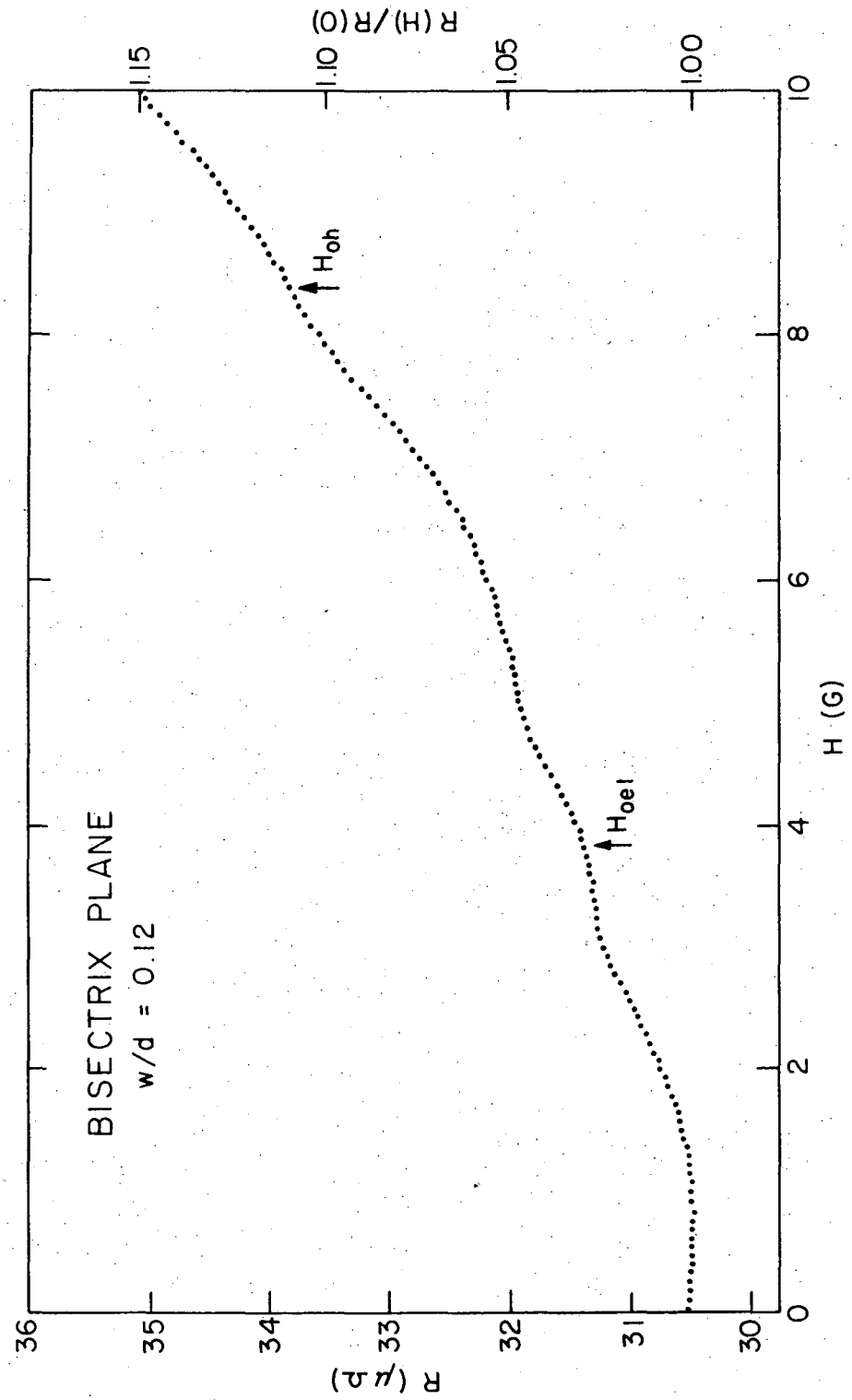

XBL 738-1720

Fig. 7

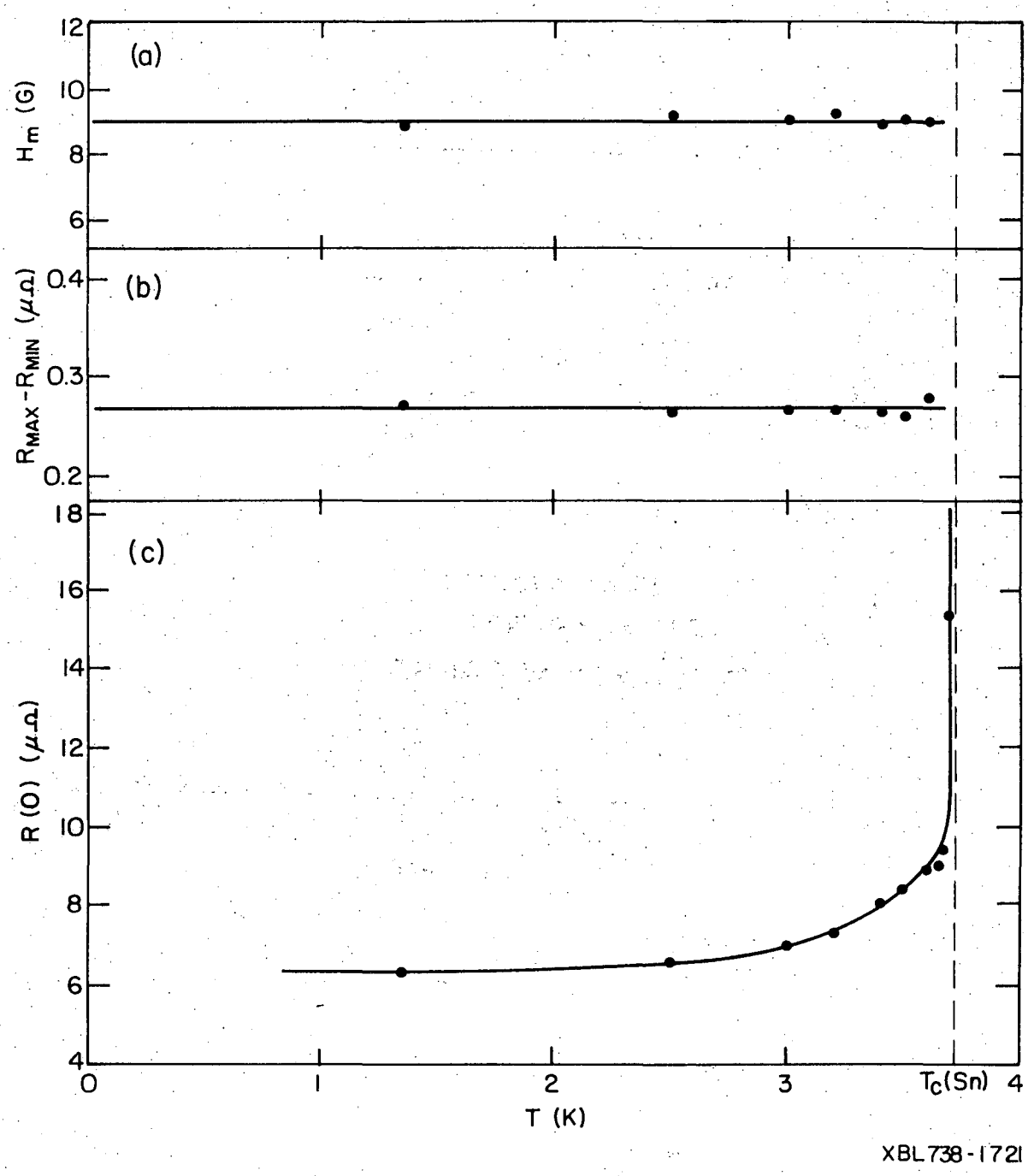

Fig. 8

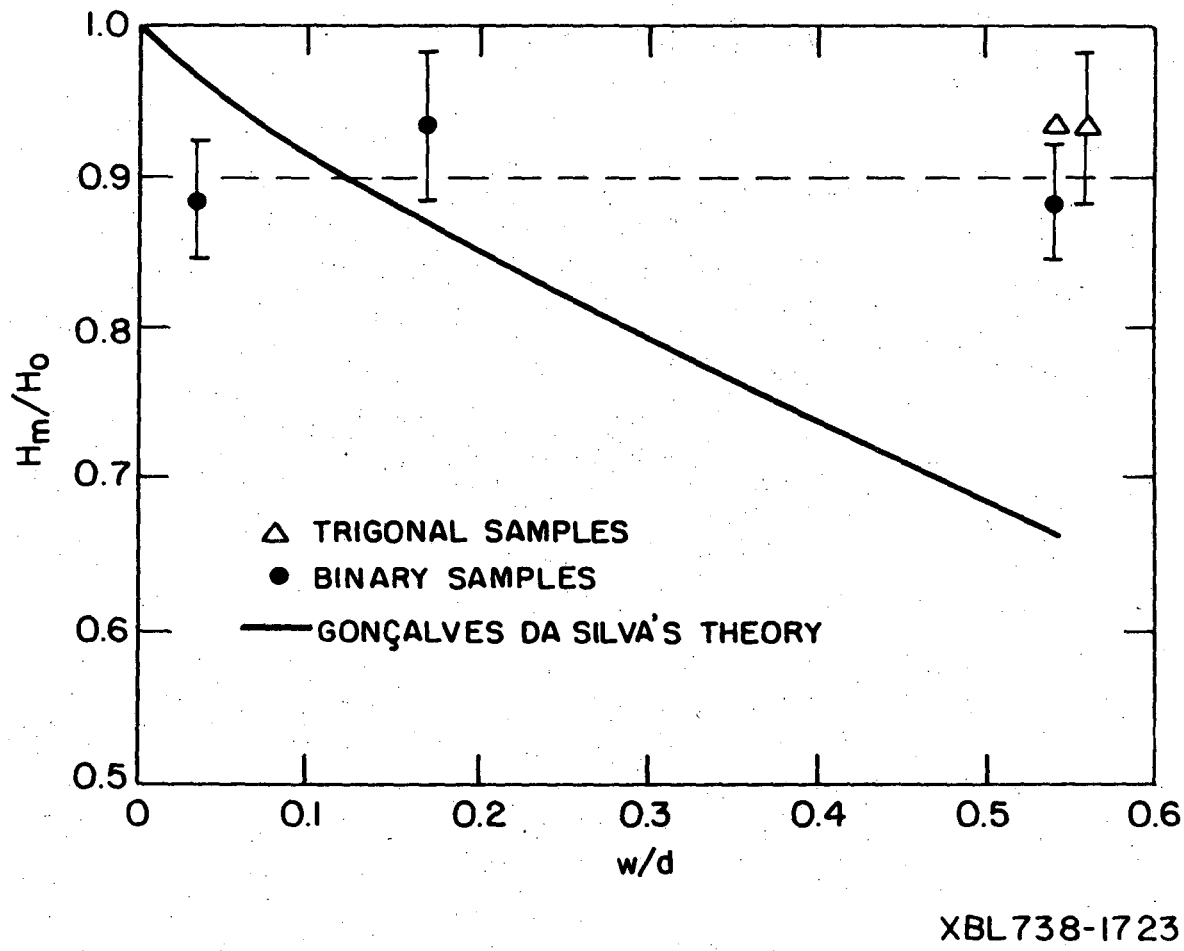
1.0
0.9
0.8
0.7
0.6
0.5
H_m/H_o
0
0.1
0.2
0.3
0.4
0.5
0.6
w/d
TRIGONAL SAMPLES
BINARY SAMPLES
GONÇALVES DA SILVA'S THEORY
XBL738-1723

Fig. 9

LEGAL NOTICE

This report was prepared as an account of work sponsored by the United States Government. Neither the United States nor the United States Atomic Energy Commission, nor any of their employees, nor any of their contractors, subcontractors, or their employees, makes any warranty, express or implied, or assumes any legal liability or responsibility for the accuracy, completeness or usefulness of any information, apparatus, product or process disclosed, or represents that its use would not infringe privately owned rights.

TECHNICAL INFORMATION DIVISION
LAWRENCE BERKELEY LABORATORY
UNIVERSITY OF CALIFORNIA
BERKELEY, CALIFORNIA 94720